Noise and Linearity of High-Speed SiGe HBT Cells in CE and CB Configuration

P. Sakalas[1,3,4], *Member IEEE*, A. Mukherjee[1], M. Schröter[1], *Senior Member IEEE*

[1]CEDIC, Technische Universität Dresden, 01062 Dresden, Germany
[3] FRL, Semiconductor Physics Institute of Center for Physical Sciences and Technology, 10257 Vilnius, Lithuania
[4] BPTI, Baltic Advanced Technology Institute, Saulėtekio al. 15, LT-10224 Vilnius, Lithuania

Abstract -- High-frequency (h.f.) noise and linearity of high-speed power cells consisting of advanced SiGe heterojunction bipolar transistors (HBTs) in common-emitter (CE) and common-base (CB) configuration were investigated. The cells features optimized metallization interconnections to reduce parasitics. DC, RF, and nonlinear large-signal characteristics as well as noise parameters were measured, simulated and analyzed. The observed low noise and output power linearity of the SiGe HBT power cells in CB operation makes them suitable for low-noise and high-frequency power applications.

Index-Terms: Compact modeling, heterojunction bipolar transistor, linearity, noise parameters, SiGe HBT.

I. INTRODUCTION

Recent advances and predictions in SiGe HBT technology [1],[2],[3] have enabled the realization of ultra h. f. low noise amplifiers, transceivers and MIMO radars [4]-[14]. Both the power amplifier and the low noise amplifier (LNA) are important components in RF transceivers. In order to increase power gain and linearity, a cascode connecting transistors in CE and CB configuration is usually used [15], with a SiGe HBT based LNA operating at 130 GHz [16]. A record frequency of 245 GHz LNA was realized in 500 GHz (DotFive) SiGe technology with a CB configuration [14]. G-band low-noise amplifiers were realized in both CE and CB operation [17], which achieved the lowest ever noise figure at 140-210 GHz frequencies [17]. LNA with CE exhibit better noise performance compared to stacked CE and CB operation LNA. The noise behavior of SiGe HBTs in different configurations was investigated in [18],[19]. It was found that the noise of first generation SiGe HBTs in CB configuration is nearly the same as in CE configuration for frequencies below 2 GHz but is higher at frequencies above 6 GHz, especially at higher collector current density [18]. The difference was explained with the noise correlation effect. In addition, the base resistance has a significant impact on $NF_{\min}$ in the CB case. However, a simplified noise model ignoring the base resistance for the first generation SiGe HBTs yields nearly same $NF_{\min}$ [19] in CE and CB configuration. The circuit design with high speed SiGe HBTs in CE, CB configuration requires exact models which captures linearity and noise behavior.

In this work, fourth generation multifinger high-speed SiGe HBT cells with optimized (i.e. reduced) base resistance in CE and CB configuration were measured, analyzed and compared using a compact model that includes the impact of noise correlation. Due to the multifinger HBT structure and respective smaller base resistance a larger $f_{\max}$ and lower noise figure (*NF*) are expected. Measured noise parameters in a wide frequency band from 8 GHz to 50 GHz, linearity and the associated analysis of a double-emitter high-speed cell in CE and CB configuration are presented.

II. DUT AND MEASUREMENT SETUP

A. HBT technology and SiGe Cell Layout Design

The investigated SiGe cells consisted of two CBE-BEBC devices connected in length direction, combined into a single cell with an emitter area A_{E0} =2x 2 x 0.13 µm x 10.16 µm. They were fabricated in the IHP SG13G2 process, which offers seven metal layers [20]. The high-speed cell layout was realized with two HBTs, separated by a shallow trench and combined into a single cell. The layout is shown in Fig. 1. The collectors and bases of the individual devices, were connected locally and terminated with *Topmetal2* of the process at the east and west side respectively. The emitter contacts, which are parallel to each other, were connected towards the vertical direction up to *Topmetal2* and finally grounded from both north and south sides.

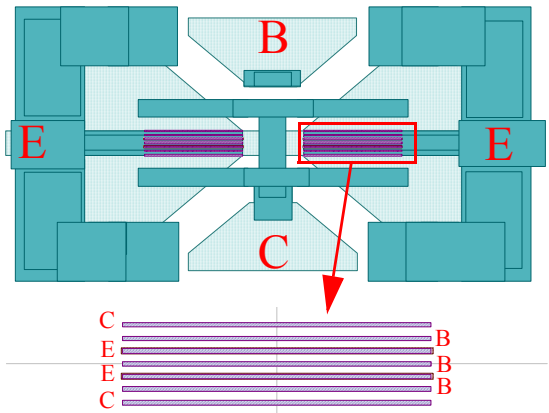

Fig. 1: Layout of embedded in RF pads 2xCBEBEBC SiGe HBT cell with grounded CE configuration.

B. Measurement equipment

On-wafer DC, RF (0.1-67 GHz), and nonlinear characteristics were measured with a PNA-X 5247A and HP4142 SMU. High-frequency noise parameters were measured with Maury Microwave Automated Tuner System ATS 5.21 07. Circuit simulations were done with

HICUM/L2 v2.34, including adjunct networks for noise correlation [21] and non-quasi static (NQS) effects [22].

III. RESULTS AND DISCUSSION

A. DC and RF characteristics

Output IV characteristic for the complete SiGe cell in CE configuration are shown in Fig. 2. Avalanche multiplication at V_{BE} = 0.74 V starts at BV_{CE0} = 1.6 V. Model parameters for both CE and CB SiGe HBTs were extracted from a set of measurements over temperature and using special tetrode structures. For $J_C(V_{CE})$ excellent agreement between model and measurement is obtained. Exceeding BV_{CEO} with the collector bias turned out to be beneficial in terms of output power and RF performance for cascode power circuits [4],[23]. Therefore, V_{CE} = 1.8 V was set as quiescent bias. Load circles with an incident RF power of -9.4 dBm are shown for both V_{CE} = 1.5 and 1.8 V. In both cases, the avalanche region is entered dynamically. Investigations show only a negligible impact of the avalanche effect on distortion. J_C increase (c. f. Fig. 2 at V_{CE} > 1.6 V) is more due to the thermal selfheating which, is a competitive mechanism to avalanche multiplication: more avalanche current turns more selfheating resulting to less avalanche current.

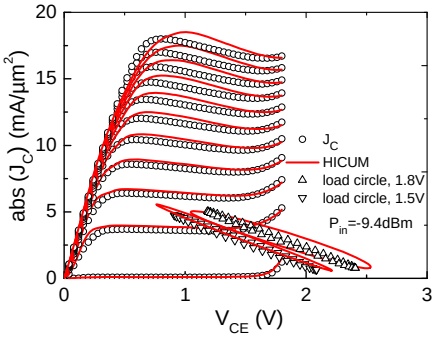

Fig. 2: Collector current density of the cell versus CE voltage with I_B drive (1 uA to 501 uA, 50 uA). Lines are HICUM.

Forward Gummel plots at V_{CE}=1.5 and 1.8 V are presented in Fig. 3. The dips in absolute value of J_B at V_{CE} = 1.8 V correspond to current reversal due to avalanche multiplication in the base-collector region. The time dependent incident V_{BE} wave at 10 GHz is also shown in order to establish a correspondence with the bias operating range.

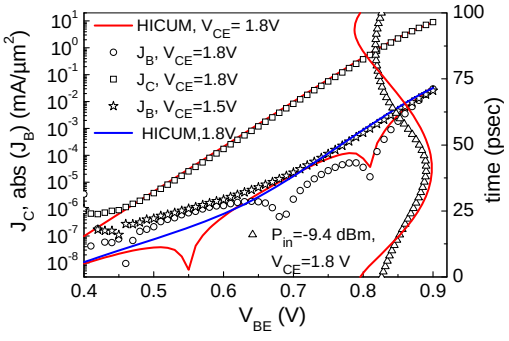

Fig. 3: Gummel plot at V_{CE} = 1.8 V, 1.5 V and V_{BE} wave at 10 GHz of incident voltage with quiescent V_{BE}= 0.84 V.

Output IV characteristics of SiGe HBT in CB configuration with I_E drive are given in Fig. 4. The current gain cut-off frequency f_T (for CE configuration only) and the maximum frequency of oscillation f_{max} versus current density are given in the Fig. 5. The f_{max} is similar for the CE and CB devices. The collector current wave in response to the incident power at 10 GHz is also shown in Fig. 5 to indicate current density swing ranges. The excellent agreement of the model with DC, RF and nonlinear characteristics in the forward active region enabled further detailed analysis of the noise behavior..

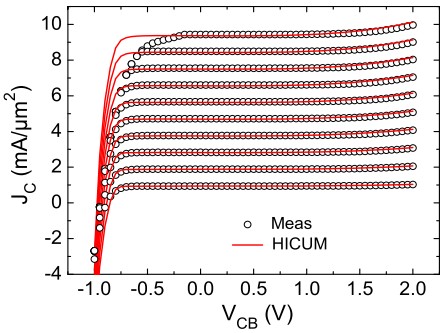

Fig. 4: Collector current density versus collector base voltage of CB SiGe HBT with emitter current drive: -50 mA to -5 mA, 5 mA step.

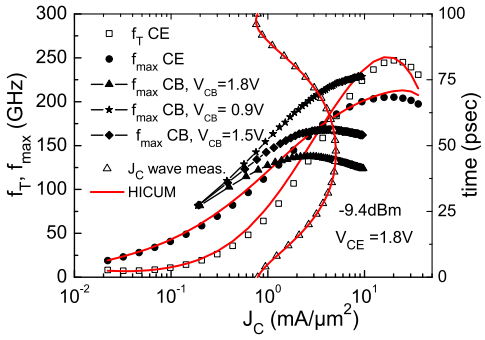

Fig. 5: Current gain cut-off frequency f_T and f_{max} over collector current density for a SiGe HBT CE and CB cells. Collector current density wave of incident power at 10 GHz is shown for CE.

B. High-frequency and power characteristics of CB and CE cells

Fig. 6: It is well known that a CB configuration HBT yields higher bandwidth at the cost of lower gain compared to a CE HBT. In the large-signal measurements, the base-emitter voltage V_{BE} was forced for the CB and CE configuration. As shown in Fig. 7, the transducer power gain G_T is slightly above 4 dB at 2 GHz and drops to 2 dB at 10 GHz. Beyond an input power of 2 dBm a frequency dependence of harmonics is observed. The SiGe HBT in CE configuration yields higher output power and G_T but at the cost of higher distortion as it is seen in Fig. 8 by the increase of the bias current density at lower P_{in} due to the even harmonics. The frequency dependence of the third harmonic was also obtained for CE configuration at 10 GHz (not shown here), confirming the lower distortion of the CB configu-

ration [24], c. f. Fig. 8, Fig. 9. one dB compression point for CE SiGe HBT at V_{CE}=1.8 V and V_{BE}=0.85 V: 1dB= -7dBm and for CB configuration more than +5 dBm..

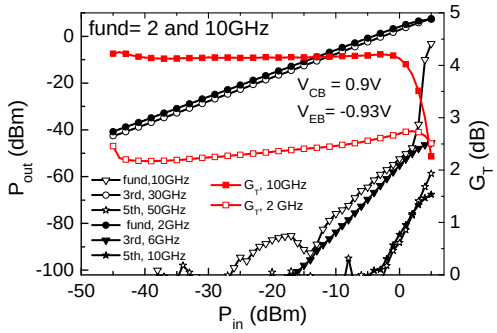

Fig. 7: Output power of fundamental (2 and 10 GHz) and harmonic frequencies versus input power of the CB cell at V_{CB}= 0.9 V and V_{EB}= -0.93 V..

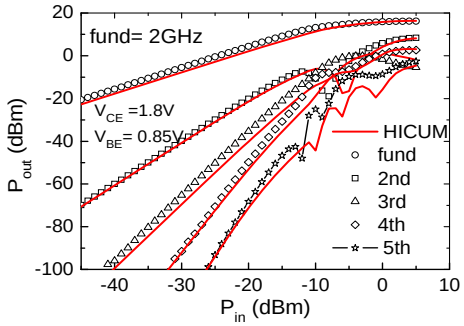

Fig. 8: Output power of fundamental (2 GHz) and harmonic frequencies versus P_{in} of the CE cell at V_{CE}=1.8 V, V_{BE}=0.85V..

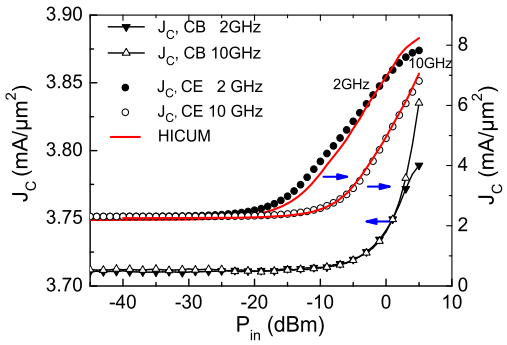

Fig. 9: $J_C(P_{in})$ at 2 and 10 GHz for the CB and CE cells, biased (CB) with V_{EB} = - 0.93 V, V_{CB} = 0.9 V, V_{CE}=1.8 V, V_{BE}=0.85V (CE).

Fig. 8 shows quiescent and dynamic current (at 2 and 10 GHz) versus input power. Frequency dependence is observed which is more pronounced in CE configuration devices.

C. High-frequency noise behavior

High-frequency noise parameters of the CE and CB cells were measured in a frequency band of 8 to 50 GHz. NF_{min} is presented in Fig. 10. The best in terms of low noise, bias points were selected to present frequency dependent noise data for CE and CB configuration devices. The comparison of NF_{min} is conditional since noise figure depends not only on the level of internal noise sources like collector current shot noise but also on transfer function or gain [21]. Therefore there is not much sense to keep same collector current in CE and CB devices and having different gain and thus transfer function to transfer noise source (collector current shot noise) to the input as defined in NF_{min} calculation. As expected for high-speed devices, fairly low noise is observed. CB devices show lower noise at lower frequencies due to lower resistance at their input port (emitter resistance) compared to the base resistance for CE device. The corresponding noise resistance R_n is around 5 Ω (CE) and 4 Ω (CB) over the measured frequency band. Such low noise resistance enables an easy impedance matching of the SiGe power cell for obtaining low-noise performance over a wide bias range. The frequency dependence of NF_{min} for CB operation is very close to that of the CE case as was observed in [18]. The impact of shot noise correlation on NF_{min} for this high-speed technology is negligible up to frequencies beyond 60 GHz.

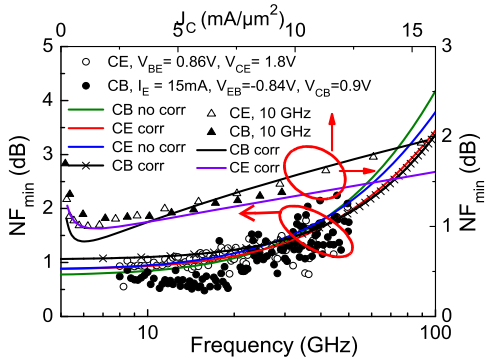

Fig. 10: Minimum noise figure NF_{min} versus frequency for SiGe CE and CB power cells. R_{BX} =6 Ω, J_C = 41 mA/μm² (for V_{BE}= 0.86 V).

The second (upper) set of curves in Fig. 10 shows the current density dependence of NF_{min}. For a fixed frequency of 10 GHz, NF_{min} within the current density range of 2... 10 mA/μm² is lower for the CB case. Noise due to avalanche multiplication was found to be negligible.

IV. CONCLUSIONS

Linearity and high-frequency noise of SiGe HBTs in common-base and common-emitter configuration were investigated. A high-speed power cell with CB configuration exhibited high linearity for 10 GHz input power and a low third harmonic (below 60 dBm at P_{in} = 0 dBm) at the cost of lower transducer power gain (4 dB) compared to a SiGe HBT in CE configuration and 25 dB power gain. Impact of avalanche multiplication on harmonic distortion was found to be negligible despite quiescent operation of about 0.2 V beyond BV_{CEO}. A dispersion of the third harmonic for both CE and CB devices was observed.

Noise parameters for a wide frequency band of 8-50 GHz were measured for both CE and CB devices. Selected bias points for frequency dependent noise parameters were used for relative comparison. A lower

NF_{min} for the CB device at lower millimeter wave frequencies was observed. The low noise figure along with a low noise resistance and relatively fair linearity enables the use of high-speed SiGe HBTs not only for low-noise applications but also for power amplifiers in cascodes at millimeter wave frequencies.

ACKNOWLEDGEMENT

This work was supported by the Ecsel project TARANTO (H2020-ECSEL-2016-1-RIA-two-stage) and the German National Science Foundation (DFG SCHR695/ 12). Everbeing Inc. is acknowledged for 300 mm probe station support.

REFERENCES

[1] P. Chevalier, et al., "Si/SiGe:C and InP/GaAsSb Heterojunction Bipolar Transistors for THz Applications", *Proc. of the IEEE*, Vol. 105, No.6, pp. 1035-1050, 2017.

[2] M. Schröter, T. Rosenbaum, P. Chevalier, B. Heinemann, S. Voinigescu, E. Preisler, J.Böck, A. Mukherjee, "SiGe HBT technology: Future trends and TCAD based roadmap", *Proc. of the IEEE*, Vol. 105, No. 6, pp. 1068-1086, 2017. B. Heinemann et al., "SiGe HBT with f_T/f_{max} of 505 GHz/720 GHz", *IEEE IEDM Technical Digest*, Dec. 2016.

[3] B. Heinemann et al. "SiGe HBT Technology with f_T/f_{max} of 300 GHz/500 GHz and 2.0 ps CML Gate Delay", *IEEE IEDM 2010,* pp.688- 691, 2010.

[4] R. B. Yishay, R. Carmon, O. Katz, D. Elad,"A high Gain Wideband 77 GHz SiGe Power Amplifier", *IEEE Radio Frequency Integrated Circuits Symposium*", pp. 529-532, 2010.

[5] M. Thian, M. Tiebout, N. B. Buchanan, V. F. Fusco, F. Dielacher, "A 76-84 GHz SiGe Power Amplifier Array Employing Low-Loss Four-way Differential Combining Transformer", *IEEE Trans. on MTT*, Vol.61, No.2, pp. 931-938, 2013.

[6] B. A. Floyd, S. K. Reynolds, U. R. Pfeiffer, T. Zwick, T. Beukema, B. Gaucher, "SiGe Bipolar Transceiver Circuits Operating at 60 GHz", *IEEE Journ. of Solid-State Circuits*, Vol. 40, No. 1, pp. 156-167, 2005.

[7] J. Böck et al., "SiGe Bipolar Technology for Automotive Radar Applications", *IEEE BCTM 4.2*, pp. 84-87, 2004.

[8] C.-H. Lin et al., "The Optimized Geometry of the SiGe HBT Power Cell for 802.11 a WLAN Applications", *IEEE Microwave and Wireless Components Letters*, Vol.17, No. 1, pp. 49-51, 2007.

[9] K. Wu, B. Fahs, M. Hella, "A 220 GHz OOK Outphasing Transmitter in 130-nm BiCMOS Technology", *IEEE BCICTS BiCMOS and Compound Semiconductor Integrated Circuits and Technology Symposium*, pp.227-230, 2018.

[10] D. Fritsche, P. Stärke, C. Carta, F. Ellinger, "A Low-Power SiGe BiCMOS 190 GHz Tranceiver Chipset with Demonstrated data Rates up to 50 Gbit/s using On-Chip Antennas", *IEEE Trans. on MTT*, Vol.65, No. 9, pp.3312-3323, 2017.

[11] M. Chang, G. M. Rebeiz, "A Wideband High-Efficiency 79-97 GHz SiGe Linear Power Amplifier with > 90 mW Output", *IEEE BCTM* 4.3, pp. 69-72, 2008.

[12] M. Sakalas, P. Sakalas, N. Joram, F. Ellinger, "Fully Differential High Input Power Handling Ultra-Wideband Low Noise Amplifier for MIMO Radar Application", *IEEE Compoud Semiconductor and Integrated Circuits Symposium, CSICS*, 2017.

[13] D. Fritsche, C. Corrado, F. Ellinger, "A Broadband 200 GHz Amplifier with 17 dB Gain and 18mW DC-Power Consumption in 0.13µm SiGe BiCMOS", *IEEE Microwave and Wireless Components Letters,* Vol.24, No. 11, pp.790-792, 2014.

[14] Y. Mao, K. Schmalz, J. Borngräber, J. C. Scheytt, "A 245 GHz CB LNA in SiGe". Proc. of the 6th *European Microwave Integrated Circuits Conference*, pp. 224-227, 2011.

[15] D. Hou, Y. -Z. Xiong, W.-Ling Coh, W. Hong, M. Madihian, "A D-Band Cascode Amplifier with 24.3 dB Gain and 7.7 dBm Output power in 0.13 µm siGe BiCMOS Technology", *IEEE Microwave and Wireless Letters*, Vol.22, No. 4, pp.191-193, 2012.

[16] B. Zhang, Y.-Z. Xiong et al., "130-GHz Gain-Enhanced SiGe Low Noise Amplifier", *IEEE Asian Solid-State Circuits Conference*, p.11.2, Beijing 2010.

[17] C. T. Coen et al., Design and On-Wafer Characterization of G-Band SiGe HBT Low-Noise Amplifiers", *IEEE MTT*, Vol.64, No.11, pp. 3631-3642, 2016.

[18] H. Li et al., "Minimum Noise Figure of SiGe HBTs under Different Operation Configurations", *Topical Meeting on Silicon Monolithic Integrated Circuits in RF Systems* (SiRF 2007), pp.56-59, 2007.

[19] H. Li Z. ,Ma, G.Niu, "Transport Shot Noise Models and NFmin Comparison for SiGe HBTs under Different Operation Configuration", *Proc. of the 2nd European Microwave Integrated Circuits Conference*", Munich, pp. 203-206, 2007.

[20] IHP SG13G2 Process Specification Rev. 0.3 (130424).

[21] J. Herricht, P. Sakalas, M. Ramonas, M. Schroter, C. Jungemann, A. Mukherjee, K. E. Moebus, "Systematic Compact Modeling of Correlated Noise in Bipolar Transistors," *IEEE Trans. on MTT*, Vol.60, No.11, pp. 3403-3412, 2012.

[22] M. Schroter, A. Chakravorty, Compact Hierarchical Bipolar Transistor Modeling with HICUM, World Scientific, p. 752.

[23] C. M. Grens, P. Cheng, J. D. Cressler, "Reliability of SiGe HBTs for Power Amplifiers--Part I: Large-Signal RF Performance and Operating Limits", *IEEE Trans. on Dev. and Material Reliability*, Vol. 9, No. 3, pp. 431-439, 2009..

[24] C. M. Grens, S. Seth, J. D. Cressler, "Common-Base Intermodulation Characteristics of Advanced SiGe HBTs", *IEEE, BCTM* 15.3, pp.244-247, 2008.